Available online at www.sciencedirect.com
SCIENCE DIRECT®

Polymer 47 (2006) 2280–2288

polymer

www.elsevier.com/locate/polymer

Radical copolymerization of *N*-vinylcarbazole and *p*-bromostyrene: determination of monomer reactivity ratios by SEC-multidetection

Audrey Lateulade, Bruno Grassl, Christine Dagron-Lartigau *, Jeanne François

LPCP-UMR5067-2, Avenue du président Angot, 64053 PAU Cedex 09, France

Received 5 July 2005; received in revised form 7 February 2006; accepted 7 February 2006

Abstract

N-Vinylcarbazole (A)/*p*-bromostyrene (B) copolymers were prepared by radical copolymerization. Size exclusion chromatography (SEC) equipped with a refractometer and UV–vis spectrophotometer was found to be a very convenient technique to follow copolymerizations and to determine monomer conversions, copolymer composition, average molecular weights, polydispersity indexes versus time. The monomer reactivity ratios r_A (*N*-vinylcarbazole) and r_B (*p*-bromostyrene) were determined by using the Finemann–Ross (FR), the inverted Finemann–Ross (IFR), the Kelen–Tüdos (KT), and the fitting curve graphical methods. The four methods were in good agreement and led to very different values for r_A (0.55) and r_B (12.3) which induces a preference for the incorporation of B in the copolymer structure. Eventually, with these results the influence of initial feed on the microstructure of the copolymer has been predicted.

Keywords: *N*-Vinylcarbazole; *p*-Bromostyrene; Copolymerization

1. Introduction

Poly(*N*-vinylcarbazole) (PA) has been widely investigated as a photoconductor and numerous studies have been reported on its photophysical properties [1–4]. As for poly(*p*-phenylene vinylene) (PPV), the use of PA in electroluminescent device began in the early 90's [5]. This is a blue-emitting polymer because of his high band gap. Moreover, the light emitting diode developed by Partridge [5] is based on double injection from the electrodes. These structures have been widely studied and their properties dramatically improved [6]. Devices in which the emitting layer was formed by blends of PA with other emissive polymers have shown strong increases in luminescence efficiency, compared to those without PA [7,8].

Synthesis of PA by classical radical polymerization has been widely studied [9–11]. Using the azoic initiator azoisobutyronitrile (AIBN) led to conventional radical polymerization while using benzoic peroxide (BPO) led to cationic and radical mechanisms [12]. Copolymerization studies based on the A monomer were performed to investigate the copolymerization mechanism as well as to determine the reactivity ratios with different comonomers. Copolymerization could be a way to improve mechanical properties of PA, in particular solubility, without altering its electrical properties.

We are involved in a series of works for the improvement of the luminescence efficiency and lifetime of electroluminescent devices. One of the strategies followed was to prepare a A/B copolymer grafted by chromophore sequences, where B is the *p*-bromostyrene (Scheme 1). It was expected that this system should provide better optoelectronic properties than a simple blend of PA with chromophore.

The present work deals with the first step (I) of preparation of this comb-like copolymer (II), whose properties will be described in subsequent papers: the A/B radical copolymerization, which at the best of our knowledge, has never been studied in the literature.

In a first place, we describe a characterization method by SEC-multidetection of a copolymerization course. In a second place, monomer reactivity ratios are determined by previously described methods, the results were compared to those obtained from a fitting method. Moreover, the determination of these parameters allowed the microstructure predictions depending on the initial feed. The aim was to determine the ability of controlling the incorporation rate of *p*-bromostyrene in the copolymer (I).

---

* Corresponding author. Tel.: +33 559 407 605; fax: +33 559 407 623.
E-mail address: christine.dagron-lartigau@univ-pau.fr (C. Dagron-Lartigau).

0032-3861/$ - see front matter © 2006 Elsevier Ltd. All rights reserved.
doi:10.1016/j.polymer.2006.02.005

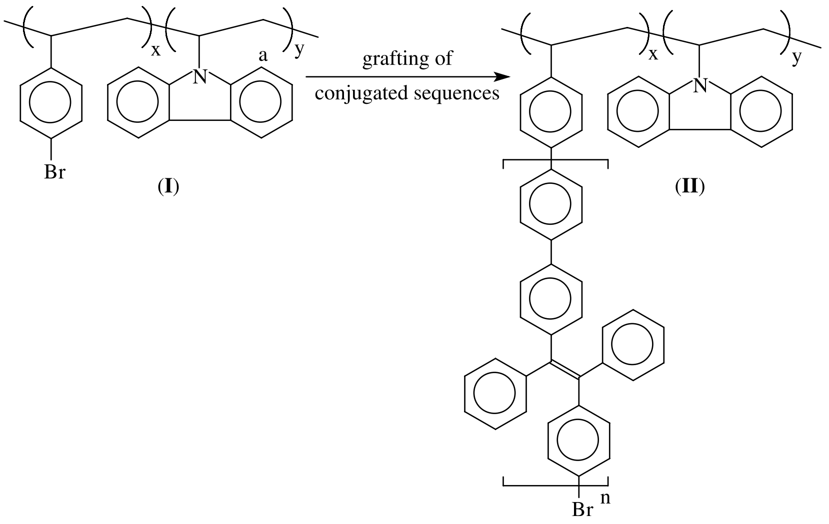

Scheme 1. Structure of A/B copolymer (I) and A/B copolymer grafted with chromophore sequences (II).

2. Experimental section

2.1. Chemicals

N-Vinylcarbazole (A, Aldrich) and azoisobutyronitrile (AIBN, Aldrich) were used as received, *p*-bromostyrene (B, Lancaster) was filtered onto basic alumina (aluminium oxide, activated, basic Brokmann I, Standard grade, ca.150 mesh, Aldrich). Tetrahydrofuran (THF) was distilled under nitrogen and filtered before use.

2.2. Equipment

Number and weight average molecular weights, $\overline{M}_n$ and $\overline{M}_w$, respectively, molecular weight distributions $\overline{M}_w/\overline{M}_n$, conversion and composition of copolymers were determined by size exclusion chromatography (SEC) using a Waters Alliance 2690 equipped with Waters Styragel HR 6, HR 4, HR 2 and HR 0,5 columns. Two detectors were used, a refractometer (RI, LED at 880 nm) and UV–vis (UV) photodiode spectrometer WATERS. RI detector was used for molecular weight measurements whereas both RI and UV detectors were used for conversion and copolymer composition determinations. The equipment was calibrated with polystyrene standards, and THF was used as eluent with 1 mL min^{-1} flow.

Compositions of copolymers solubilized in $CDCl_3$ were also determined by ^{1}H NMR experiments using a spectrometer Bruker Avance AM400.

UV–vis measurements were carried out using a Shimadzu 2101-PC spectrometer, cells in quartz and spectral windows between 200 and 600 nm with resolution of 0.1 nm.

2.3. Polymerization

2.3.1. Homopolymerization

Radical homopolymerizations were carried out in solution either in THF or in bulk (Table 1). *N*-Vinylcarbazole (or *p*-bromostyrene), THF (for solution experiments only) and AIBN (0.005 equiv) were introduced in a 50 mL Schlenck vessel under gentle nitrogen purge throughout the reaction medium. The reaction mixture was then heated up to 60 °C for several hours.

Table 1
Homopolymerization of *N*-vinylcarbazole and *p*-bromostyrene in presence of AIBN in THF solution and in bulk

mA (g)	[A] (mol L^{-1})	mB (g)	[B] (mol L^{-1})	[AIBN] (mol L^{-1})	Time of polymerization (h)	Conversion (%)	$\overline{M}_n$[a] (g mol^{-1})	$\overline{M}_w/\overline{M}_n$[a]
0.483	1.09	0	–	0.006	1.5	49	6100	1.7
					2	66	6010	
					3	87	6150	
					4	92	6290	
0	–	0.388	1.06	0.008	1	6	5100	3.7
					1.5	21	5040	
					2.5	28	5170	
					3.5	36	5200	
0.252	–	0	–	0.003	1	17	144,500	1.8
0	–	0.222	–	0.003	1	31	94,600	1.6

[a] Results obtained from SEC experiments against PS standards.

The thermal homopolymerizations were carried out in bulk. A 50 mL Schlenck vessel was charged with *N*-vinylcarbazole (or *p*-bromostyrene) under gentle nitrogen purge and heated up to 140 °C (in the case of A) or 125 °C (in the case of B) for several hours. The polymerizations were stopped by cooling in liquid nitrogen. The homopolymers were precipitated twice from methanol and dried in vacuum. Conversions were determined gravimetrically and molecular weights were obtained by SEC (RI detector, against PS standards) in THF (PA: $\overline{M}_n = 55\times10^3$ g mol^{-1}, $\overline{M}_w/\overline{M}_n = 3.5$; PB: $\overline{M}_n = 96\times10^3$ g mol^{-1}, $\overline{M}_w/\overline{M}_n = 2.2$).

2.3.2. Copolymerization

The bulk copolymerizations were carried out in 50 mL a Schlenck vessel under gentle nitrogen purge throughout the reaction medium. The Schlenck was then charged with *N*-vinylcarbazole, *p*-bromostyrene and AIBN (0.015 equiv) and heated up to 60 °C for 1 h or less to obtain low yields ($R<10\%$). The polymerization medium was then analyzed by SEC-multidetection. Conversion, composition and molecular weight were determined for each sample.

Copolymers were precipated four times in methanol and dried under vacuum before analysis by ^{1}H NMR.

3. Copolymerization studies by SEC with double detector

3.1. Principle of the method

In the analysis of copolymers and comonomer mixtures, the use of multiple detection is necessary and almost inevitable. When the response factors of the detectors for polymer components are different enough, chemical composition along the molecular weight distribution can be determined from detector signals. Usually, a combination of UV and RI detection is used, but other detector combinations have also been described [13]. If the copolymer components have different UV spectra, a diode array detector is an instrument of choice. In the case of non-UV absorbing polymers, a combination of RI and density detection gives the desired information on chemical composition [14]. The technique can also be applied to oligomers instead of compensating for the molecular weight dependence of detector response.

3.2. Elution of a monomer or a homopolymer

In the simply case of the injection of a monomer or a homopolymer in a chromatographic column, the signals of the two detectors (Δn_i and A_i for the refractometer and UV spectrometer, respectively) are proportional to C_i, the instantaneous mass concentration (mg ml^{-1}) for each elution volume v_i:

$$\mathrm{RI}: \Delta n_i = K_{\mathrm{RI}}(\mathrm{d}n/\mathrm{d}c)C_{\mathrm{i}} \tag{1}$$

$$\mathrm{UV}: A_{\mathrm{i}} = K_{\mathrm{UV}}\varepsilon C_{\mathrm{i}} \tag{2}$$

where K_{RI} and K_{UV} are the instrumental constants of the refractometer and UV–vis spectrometer, respectively, (dn/dc) is the refractive index increment of the solute, ε is the absorption coefficient of the sample.

Besides the surfaces of the chromatographic peaks (S_{RI} or S_{UV}) are proportional to the total amount of injected mass m, if the totality is eluted.

If there is no retention on the column, it is possible to determine the (dn/dc) or ε values, from the known value of m:

$$\left(\frac{\mathrm{d}n}{\mathrm{d}c}\right) \propto \frac{S_{\mathrm{RI}}}{K_{\mathrm{RI}}m} \tag{3}$$

$$\varepsilon \propto \frac{S_{\mathrm{UV}}}{K_{\mathrm{UV}}m} \tag{4}$$

This method was used to determine the (dn/dc) and ε values of both A and B monomers ((dn/dc)$_{\mathrm{A}}$, (dn/dc)$_{\mathrm{B}}$ and ε_{A}, ε_{B}) and both PA and PB homopolymers ((dn/dc)$_{\mathrm{PA}}$, (dn/dc)$_{\mathrm{PB}}$ and $\varepsilon_{\mathrm{PA}}$, $\varepsilon_{\mathrm{PB}}$). The values of K_{RI} and K_{UV} were previously determined by using polystyrene standards of well known (dn/dc) and ε, and by applying the same expressions (3) and (4) (Fig. 1). The Fig. 1 gives the variations of RI and UV peak areas versus the injected mass (since various concentrations and injection volumes were used). That only linearities are obtained, a good correlation was concluded on the determination of K_{RI} and K_{UV}. The flow injection analysis described in the literature [14], involving the sample injections directly through injector into the detector, thus bypassing the columns (or using short columns) was not used. An independent determination of PS (dn/dc) was carried out by automatic continuous mixing technique described by Thévenot et al. [15] and by performing a stepped-concentration gradient monitoring experiments using different PS batch solutions described by Brousseau et al. [16]. With this technique a (dn/dc) of 0.190 mL g^{-1} was found for PS in THF at room temperature (RI detector) [17]. The validity of this approach was tested by comparing the injected mass of SEC runs with the calculated mass. Fig. 1 shows the calibration curve, from which $K_{\mathrm{RI}} = 16\times10^9$ mL^{-1} was determined. The constant K_{UV} was determined through the calibration of the UV

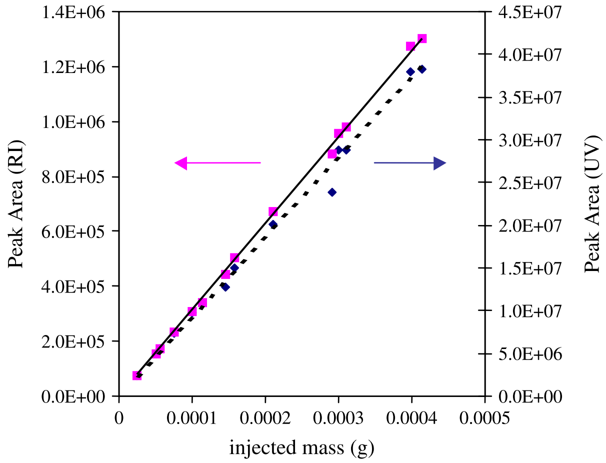

Fig. 1. Determination of the constant of the apparatus from a standard polystyrene; (■) RI detection; (♦) UV detection; (dn/dc) = 0.1902 mL g^{-1} and $\varepsilon = 1.652$ g^{-1} L cm^{-1}.

detector with the same standards of known absorption coefficient.

3.3. Elution of a monomer mixture or a copolymer

In the case of a binary mixture of comonomers (A and B), the detector signals are the sum of the contribution of each monomer:

$$\Delta n_i = K_{\mathrm{RI}}\left[\left(\frac{\mathrm{d}n}{\mathrm{d}c}\right)_{\mathrm{A}} C_{\mathrm{A},\,i} + \left(\frac{\mathrm{d}n}{\mathrm{d}c}\right)_{\mathrm{B}} C_{\mathrm{B},\,i}\right] \tag{5}$$

$$A_i = K_{\mathrm{UV}}\left[\varepsilon_{\mathrm{A}} C_{\mathrm{A},\,i} + \varepsilon_{\mathrm{B}} C_{\mathrm{B},\,i}\right] \tag{6}$$

The concentration of each component at an elution volume v_i can easily be determined by resolving Eqs. (5) and (6), provided $(\mathrm{d}n/\mathrm{d}c)_{\mathrm{A}}$, $(\mathrm{d}n/\mathrm{d}c)_{\mathrm{B}}$, ε_{A}, ε_{B}, K_{RI} and K_{UV} are known. The same equations can be written for a copolymer, but the refractive index increment and the absorption coefficient are those of the monomer units in the copolymer. We have assumed that the optical properties of the monomer units in the copolymer and in their homopolymers are identical. This means that we have used the values of $(\mathrm{d}n/\mathrm{d}c)_{\mathrm{PA}}$ and $\varepsilon_{\mathrm{PA}}$, $(\mathrm{d}n/\mathrm{d}c)_{\mathrm{PB}}$ and $\varepsilon_{\mathrm{PB}}$ for the respective contribution of A and B monomer units.

3.4. Elution of a reaction mixture

The samples from the reaction medium at various copolymerization times contain: the unreacted monomers and the copolymer. If the molecular weight of the copolymer is high enough, two peaks are obtained with each detector, corresponding respectively, to monomer mixture (peak 1) and copolymer (peak 2). An example of such chromatograms is given in Fig. 2.

Though, the surfaces of the refractometric peaks 1 and 2 are the following:

$$S_{\mathrm{RI1}} \propto K_{\mathrm{RI}}\left[\left(\frac{\mathrm{d}n}{\mathrm{d}c}\right)_{\mathrm{A}} m_{\mathrm{A}} + \left(\frac{\mathrm{d}n}{\mathrm{d}c}\right)_{\mathrm{B}} m_{\mathrm{B}}\right] \tag{7}$$

$$S_{\mathrm{RI2}} \propto K_{\mathrm{RI}}\left[\left(\frac{\mathrm{d}n}{\mathrm{d}c}\right)_{\mathrm{PA}} m_{\mathrm{PA}} + \left(\frac{\mathrm{d}n}{\mathrm{d}c}\right)_{\mathrm{PB}} m_{\mathrm{PB}}\right] \tag{8}$$

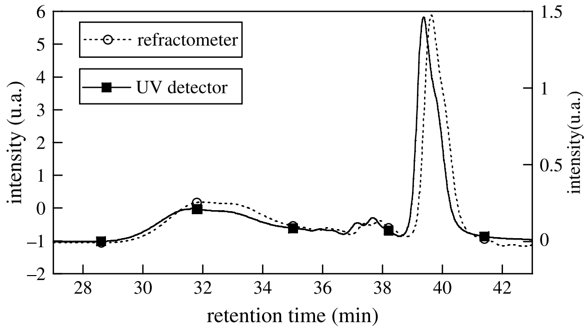

Fig. 2. Chromatograms of mixture of copolymer and monomers obtained with UV-detector and refractometer.

and the surfaces of the UV peak are:

$$S_{\mathrm{UV1}} \propto K_{\mathrm{UV}}\left[\varepsilon_{\mathrm{A}} m_{\mathrm{A}} + \varepsilon_{\mathrm{B}} m_{\mathrm{B}}\right] \tag{9}$$

$$S_{\mathrm{UV2}} \propto K_{\mathrm{UV}}\left[\varepsilon_{\mathrm{PA}} m_{\mathrm{PA}} + \varepsilon_{\mathrm{PB}} m_{\mathrm{PB}}\right] \tag{10}$$

where m_{A}, m_{B}, m_{PA} and m_{PB} are the injected masses of monomer A, monomer B, monomer units A and B in the copolymer, respectively.

Furthermore, the copolymerization conversion R can be obtained with:

$$R = \frac{m_{\mathrm{PA}} + m_{\mathrm{PB}}}{m_{\mathrm{A}} + m_{\mathrm{B}} + m_{\mathrm{PA}} + m_{\mathrm{PB}}} \tag{11}$$

and the comonomer ratio with:

$$F = \frac{m_{\mathrm{PA}} M_{\mathrm{B}}}{M_{\mathrm{A}} m_{\mathrm{PB}}} \tag{12}$$

where M_{A} and M_{B} are, respectively, the molecular weight of A and B units in the copolymer.

3.5. Choice of the wavelength for UV–vis detection

Fig. 3 shows the UV–vis spectra of the species A, B, PA and PB. In the range of wavelength between 300 and 360 nm, *p*-bromostyrene (B) and poly(*p*-bromostyrene) (PB) do not absorb, whereas *N*-vinylcarbazole (A) and its homopolymer (PA) exhibit two peaks and a shoulder. The wavelength for UV–vis detection was set at 340 nm, at the maximum value. Though, Eqs. (9) and (10) are simplified since second terms are equal to zero.

4. Results and discussion

4.1. The homopolymers

4.1.1. Molecular weights and polydispersity index

Table 1 compares the characteristics of PA and PB homopolymers obtained either in THF solutions or in bulk. The first one exhibited low molecular weight below 10^4 g mol^{-1}, which was due to radical transfer to THF. We have indeed determined the transfer constant to solvent in the polymerization *p*-bromostyrene and *N*-vinylcarbazole in THF

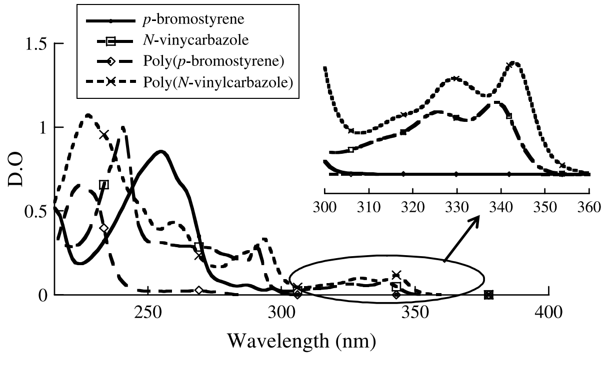

Fig. 3. UV–vis spectra of B (−), A (□) PB (◇) and PA (×) in THF.

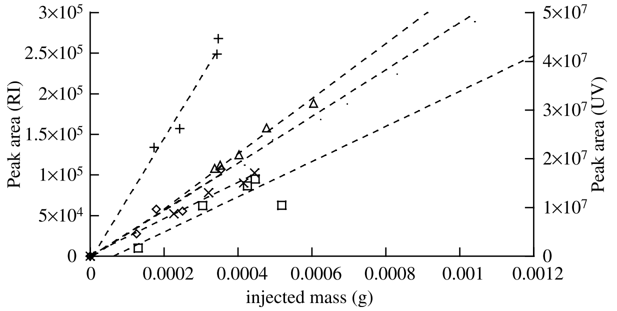

Fig. 4. Evolution of peak areas of chromatograms with RI and UV detectors of A (×)RI detection; (+) UV detection), PA (□) RI detection; (Δ) UV detection) B (◇) RI detection) and PB ((○) RI detection) with injected mass in the column (*g*).

(equal to 0.12 and 0.54, respectively). Besides, the molecular weight distribution was very different for PA and PB, with a broader one of PB. The polydispersity index of PA (1.7) was in the range expected for a radical polymerization.

Furthermore, in the case of the copolymerization in bulk, the molecular weight distribution was higher than that expected with classical radical polymerization and was between 2.2 and 2.9.

4.1.2. (dn/dc) and ε

Solutions of monomers and homopolymers of various concentrations issued from thermal polymerizations were injected in the SEC columns.

Fig. 4 shows the variations of the refractometric and UV peak areas as function of the injected mass. Straight lines were obtained and the values of ε at 340 nm and (d*n*/d*c*) determined from their slopes are reported in Table 2. A difference of (d*n*/d*c*) is observed between B and PB whereas the same values were obtained for A and PA. Homopolymerizations in THF were carried out to prepare A and B oligomers in order to check the influence of molecular weight on refractive properties of these polymers. In fact, no significant difference was found between (d*n*/d*c*) values of oligomers and polymers. One can deduce that the decrease of (d*n*/d*c*) between B and PB occurs only for very small oligomerization degree. Such a variation of refractive indexes could be neglected in the analyses of the results. Some experimental works showed a significant dependence of molecular weight on refractive indexes in the range $M < 10^4$, this effect is further discussed (cf. Section 4.2.2). However, the variations were found to be strongly dependent on the nature of the end groups and may be negligible if the refractive index of these end groups is close to the one of the central monomer units.

Table 2
Refractive index increment and coefficient absorption at 340 nm for A, PA, B and PB

	A	PA	B	PB
ε_{340} (cm^2 g^{-1})	22.9	10.4	$<2\times10^{-4}$	$<1\times10^{-4}$
$(\partial n/\partial c)$(mL g^{-1})	0.180	0.180	0.141	0.135

Table 3
Monomer composition in the initial feed and copolymer compositions at low conversion

f_A	f_B	F_A	F_B	Conversion (%)
0.51	0.49	0.13	0.87	<10
0.51	0.49	0.11	0.89	<10
0.32	0.68	0.04	0.96	<10
0.32	0.68	0.03	0.97	<10
0.77	0.23	0.41	0.59	<10
0.04	0.96	0.01	0.99	<10

4.2. The copolymers

4.2.1. Reactivity ratios

Several copolymerization experiments in bulk with different initial feed of B were carried out to determinate r_A and r_B. Sampling was made as a function of time and after dilution in THF the aliquots were injected in SEC columns. The summarized results of SEC analyses presented in Table 3 showed that for low conversion, the copolymer composition was dramatically different from the initial feed, with a higher incorporation of B. Assuming that the reactivity ratios are only dependent on the terminal group and making the steady-state of radical species assumption, one can obtain the differential copolymerization Eq. (13) given by Lewis and Mayo [18].

$$F_A = \frac{r_A f_A^2 + f_A f_B}{r_A f_A^2 + 2 f_A f_B + r_B f_B^2} \tag{13}$$

where F_A is the instantaneous molar fraction of A in the copolymer, f_A and f_B the molar fraction of A and B in the initial feed, respectively.

Because this equation is only valid if the variation of the reaction medium composition is low, particular attention was focused on having a conversion below 10%. The reactivity ratios are related to the different rate constants of the copolymerization k_{ij} by:

$$r_A = \frac{k_{AA}}{k_{AB}} \tag{14a}$$

$$r_B = \frac{k_{BB}}{k_{BA}} \tag{14b}$$

In this work, the monomer reactivity ratios were determined by three linear methods: the Finemann–Ross (FR) [19], the inverted Finemann–Ross (IFR) [19], the Kelen–Tüdos (KT) [20] and the data processing method.

According to the FR method the monomer reactivity ratios were obtained by the Eq. (15):

$$X = \frac{1 + r_A x}{1 + r_B / x} \tag{15}$$

The parameters X and x are defined as follows:

$$X = \frac{d[A]}{d[B]} = \frac{F_A}{F_B} \tag{16}$$

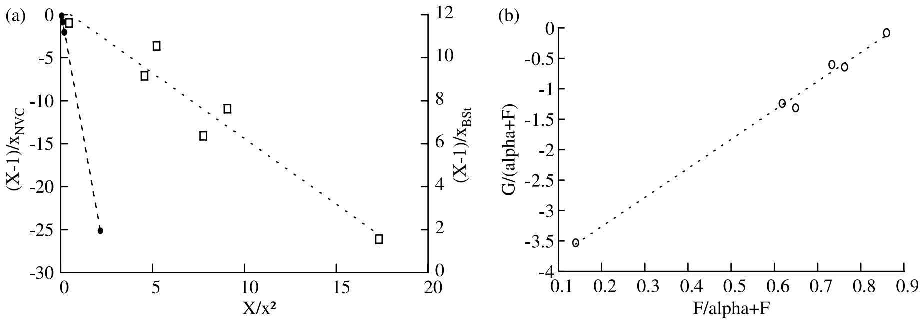

Fig. 5. Graphical determination of reactivity ratios (a) Finemann–Ross (●) and inverted Finemann–Ross (□); (b) Kelen–Tüdos methods.

$$x=\frac{[\mathrm{A}]}{[\mathrm{B}]}=\frac{f_{\mathrm{A}}}{f_{\mathrm{B}}} \tag{17}$$

which lead to:

$$\frac{X-1}{x}=r_{\mathrm{A}}-r_{\mathrm{B}}\frac{X}{x^2} \tag{18}$$

The plot of $(X-1)/x$ versus (X/x^2) gave a straight line whose slope is $-r_{\mathrm{B}}$ and the intercept is r_{A}.

The inverted FR method is based on the same equation by permuting the two monomers. In this method, the plot of $(X-1)/x$ versus (X/x^2) gave r_{A} from the slope and r_{B} from the intercept. The plots are reported in Fig. 5(a) and the reactivity ratios are given in Table 4.

Alternatively the reactivity ratios can be obtained using the KT method which is based on the equation:

$$\eta=\left(r_{\mathrm{A}}+\frac{r_{\mathrm{B}}}{\alpha}\right)\xi-\frac{r_{\mathrm{B}}}{\alpha} \tag{19}$$

$$\eta=\frac{G}{\alpha+F} \tag{20a}$$

and

$$\xi=\frac{F}{\alpha+F} \tag{20b}$$

where η and ξ are functions of the parameters G and F: with

$$G=\frac{x(X-1)}{X}=x-\frac{x}{X} \tag{21a}$$

and

$$F=\frac{x^2}{X} \tag{21b}$$

Table 4
Reactivity ratios for the A/B copolymerization from Finemann–Ross, inverted Finemann–Ross, Kelen–Tüdos methods and the fitting method

Method	r_{A}	r_{B}
FR	0.52	11.85
IFR	0.56	12.09
KT	0.54	13.49
Curve fit	0.59	11.89

and α a constant which is equal to $\sqrt{F_{\min}F_{\max}}$, $F_{\min}$ and $F_{\max}$ being the minimum and the maximum F values, respectively, from the series of measurements.

From the linear plot of η as a function of ξ, the values of η for $\xi=0$ and $\xi=1$ are used to calculate the reactivity ratios according to the Eqs. (22) and (23) (Fig. 5(b) for the plot).

$$\text{if } \xi=0 \text{ then } \eta=-\frac{r_{\mathrm{B}}}{\alpha} \tag{22}$$

and

$$\text{if } \xi=1 \text{ then } \eta=r_A \tag{23}$$

Actually, the data processing method used was a fitting (Fig. 6) of the plot $F_{\mathrm{A}}=f(f_{\mathrm{A}})$ by plotting a curve with the following equation:

$$y=\frac{r_{\mathrm{A}}f_{\mathrm{A}}^2+f_{\mathrm{A}}(1-f_{\mathrm{A}})}{r_{\mathrm{A}}f_{\mathrm{A}}^2+2f_{\mathrm{A}}(1-f_{\mathrm{A}})+r_{\mathrm{B}}(1-f_{\mathrm{A}})^2} \tag{24}$$

The monomer reactivity ratios obtained from the four methods are summarized in Table 4.

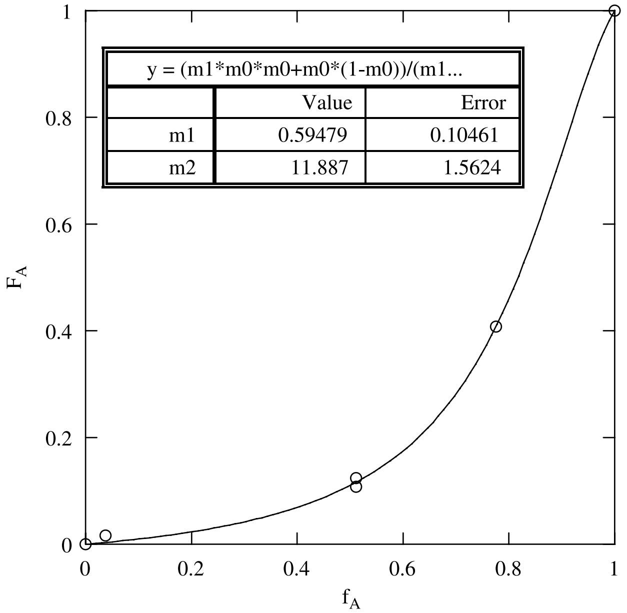

y = (m1*m0*m0+m0*(1-m0))/(m1...

	Value	Error
m1	0.59479	0.10461
m2	11.887	1.5624

Fig. 6. Composition curve of A/B copolymers synthesized with AIBN at 60 °C and results of the fit.

Table 5
Reactivity ratios for copolymers described in literature system

System	r_1	r_2	Temperature (°C)	Reference
N-Vinylcarbazole/styrene	0.012	5.5	70	[18,19]
	0.035	5.7	75	[20]
	0.062	5.6	60	[21]
N-Vinylcarbazole/*p*-Chlorostyrene	0.023	7	30	[22]

4.2.2. Discussion of the method

Good agreement was found with the data obtained from the four methods. The easiest method to perform was the data processing method and afforded good results. So we decided to choose this method for determining reactivity ratios. Moreover, we showed that determining reactivity ratios by SEC is easy and fast as soon as one of the polymers and one of the monomers exhibit different absorption peaks with UV/vis detector. For comparison, we present in Table 5 the reactivity ratios of *N*-vinylcarbazole/styrene and *N*-vinylcarbazole/*p*-chlorostyrene copolymers found in literature [21–25]. We can see that these values are comparable to those calculated for the copolymer A/B.

This method of characterization is interesting since (d*n*/d*c*) and ε were easily determined for monomers and polymers. Besides, a great reproducibility of the results was observed.

Moreover, considering the weak absorption of B at 340 nm, the peak areas of A and B of the chromatograms obtained with UV–vis detection were compared. The peak area for B was 450 times lower than peak area for A. It corresponded to an error of 2/1000, so the absorbance of B was neglected.

Effect of temperature over (d*n*/d*c*) has not been studied, but the room was thermostated to limit the temperature effect over columns behaviour. Moreover, characterizations were carried out on the same apparatus, with the same solvent (THF), columns were at the same temperature, refractometer thermostated at 40 °C and UV–vis detector at room temperature.

Besides, it was difficult to compare the values obtained with those given in literature. In fact, they are dependent on the temperature, the wavelength, the molecular weight of oligomers [26] with $\overline{M}_n < 2\times10^4$ g mol^{-1}and the process used, so a great variation in values is observed in literature [27,16]. Thus, it was not surprising that the values in literature for PA were between 0.262 and 0.282 [17]. They were given in the same conditions of temperature and samples (equivalent molecular weights) but at different wavelengths. Our results were an average of the attempts for all the wavelengths, and so, difficult to compare with those obtained in the literature.

RI detector measures a property of the entire eluate, that means, it is sensitive towards a specific refractive-index increment of the sample. This is a well-known fact that specific properties are related to molecular weight *M*, as shown in Eq. (25):

$$\left(\frac{dn}{dc}\right) = \left(\frac{dn}{dc}\right)_\infty + \frac{K}{M} \tag{25}$$

where $(\mathrm{d}n/\mathrm{d}c)_\infty$ is the specific refractive-index increment of a polymer with infinite (or at least very high) molecular weight, and *K* is a constant reflecting the influence of the end groups.

In a plot of (d*n*/d*c*) versus molecular weight M_i of a homologous polymer series (with the same end groups) one will obtain a straight line with the intercept $(\mathrm{d}n/\mathrm{d}c)_\infty$ (the response factor of a polymer with very high molecular weight, or the response factor of the repeating unit) and the slope *K*, which represents the influence of the end groups. Different methods can be applied for the determination of $(\mathrm{d}n/\mathrm{d}c)_\infty$ and *K*. If a sufficient number of monodisperse polymers are available (as is the case with PS standard), linear regression will be the method of choice. Once $(\mathrm{d}n/\mathrm{d}c)_\infty$ and *K* are known, the correct response factors for each fraction eluting from a SEC column can be calculated (with the molecular weight obtained from the SEC calibration).

In our study, the effect of the molecular weight on the refractive index increment was determined and the same values were obtained for polymers with molecular weights between 10^3 and 180×10^3 g mol^{-1} with an error of $\pm5\times10^{-4}$. Furthermore, values obtained for A and PA were close. Polymer with low molecular weights were obtained as it was previously said, in presence of a transfer agent: THF.

It was also supposed that the microstructure of the copolymers did not influenced the increment determination. To verify this hypothesis results obtained by ^{1}H NMR and SEC were compared.

With ^{1}H NMR spectrum it was possible to determine copolymer composition (Fig. 7). The copolymers were purified by several precipitations from methanol. The reference of chemical shifts (δ) was chloroform at 7.27 ppm. Moreover, water included in $CDCl_3$ exhibits a chemical shift at 1.6 ppm (singlet). The composition was determined as so on: multiplets at 6.35, 7.10, and 7.9 ppm were attributed to aromatic protons of *p*-bromostyrene and *N*-vinylcarbazole aromatic rings, except proton Ha of A unit (Scheme 1) which resonated at 4.95 ppm (multiplet) [28,29] Fig. 7.

The composition of A (F_A) in the copolymer could be expressed as Eq. (26):

$$F_A = \frac{y}{x+y} = \frac{4I_{4.95}}{I_{6.35}+I_{7.10}+I_{7.9}-3I_{4.95}} \tag{26}$$

with $I_{4.95}$: integration value of the aromatic proton Ha of A units at 4.95 ppm.

$I_{6.35}, I_{7.1}, I_{7.9}$: integration value of the other aromatic protons of A and B units at 6.35, 7.1 and 7.9 ppm.

In these conditions, the fraction of A in the copolymer was found to be $F_A = 0.47$ by ^{1}H NMR and $F_A = 0.41$ by SEC-multidetection. We quantified the peak area of the reference (chloroform) since it was included in the multiplet of aromatic protons. It was found that the chloroform moiety was about 3%, so in the given results its contribution was neglected. So compositions obtained by both methods NMR and SEC were in good agreement. Nevertheless, in our study, the characterization by SEC, giving molecular weights, distribution of molecular

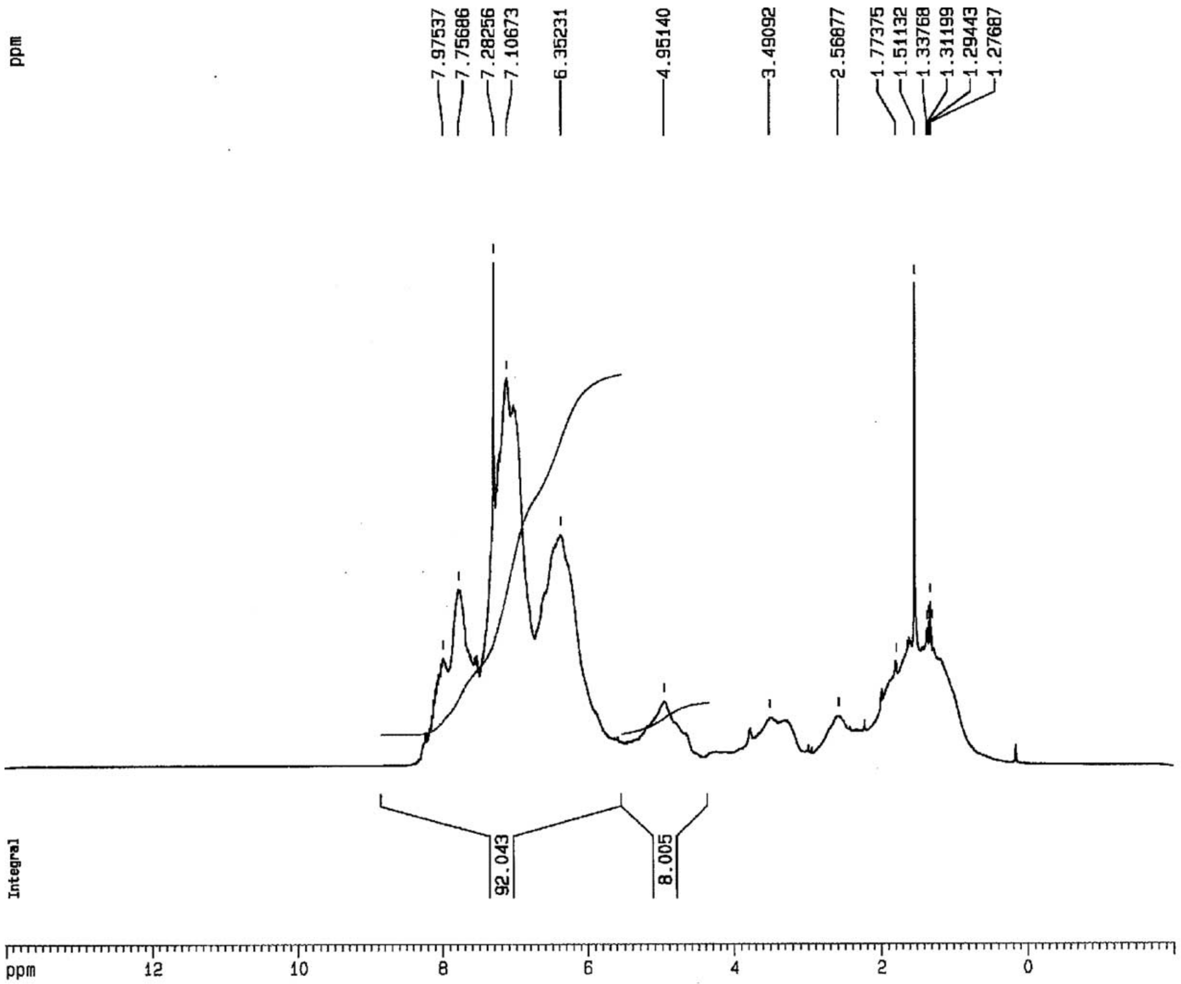

Fig. 7. ^{1}H NMR spectrum of poly(*N*-vinylcarbazole-*stat*-*p*-bromostyrene) in $CDCl_3$ (400 MHz).

weights, conversion and copolymer compositions without further purification was more convenient than NMR technique.

4.2.3. Microstructure of the copolymers

To optimize electroluminescent properties of emissive materials, it is necessary to provide exciton confinement by avoiding π-stacking of conjugated sequences. Though, in our comb-like copolymers, the knowledge of reactivity ratios allowed us to find the accurate conditions of initial feed for limiting long sequences of B.

Provided that a growing chain with a terminal radical $A^{\cdot}$ can react either with a A unit or a B unit, the respective probability is p_{AA} and p_{AB} with the corresponding rates v_{AA} and v_{AB}:

$$p_{AA} = \frac{v_{AA}}{v_{AA} + v_{AB}} = \frac{k_{AA}[A^{\cdot}][A]}{k_{AA}[A^{\cdot}][A] + k_{AB}[A^{\cdot}][B]} = \frac{r_A f_A}{r_A f_A + f_B} \tag{27a}$$

$$p_{AB} = \frac{v_{AB}}{v_{AA} + v_{AB}} = \frac{k_{AB}[A^{\cdot}][B]}{k_{AA}[A^{\cdot}][A] + k_{AB}[A^{\cdot}][B]} = \frac{f_B}{r_A f_A + f_B} \tag{27b}$$

and $p_{AA} + p_{AB} = 1$

The same calculations can be done from B unit:

$$p_{BB} = \frac{BfB}{r_B f_B + f_A} \tag{28a}$$

$$p_{BA} = \frac{f_A}{r_B f_B + f_A} \tag{28b}$$

In our case, as we want to limit long sequences of B units, we have calculated the probability to form a sequence with n B units, comprising at each end one A unit is:

$$pB_n = np_{BB}^{(n-1)} p_{BA} = np_{BB}^{(n-1)} (1 - p_{BB}) \tag{29}$$

The plot pB_n versus n clearly shows the distribution of B sequence lengths for different initial feed (Fig. 8). From these results and from the determination of the mean number of

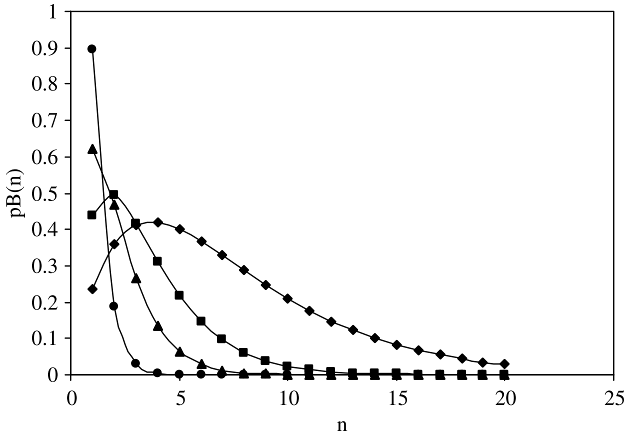

Fig. 8. Distribution of B sequence lengths for different initial B fraction (f_B); (◆) 0.22, $\bar{n}=4.24$; (■) 0.1, $\bar{n}=2.28$; (▲) 0.05, $\bar{n}=1.60$ (●) 0.01, $\bar{n}=1.12$.

sequence lengths ($\bar{n}=1/p_{BA}$) given in Fig. 8, we can see that the molar fraction of B in the initial feed should be no higher than 5%. In that condition, the highest probability is to form B sequences with a single unit. It should be noted that all the calculations are valid for a conversion below 10%. For our aimed diode application, this low conversion is overcome by the high-value of the final grafted material.

5. Conclusion

Copolymers of *N*-vinylcarbazole and *p*-bromostyrene were prepared by classical radical polymerization at 60 °C with AIBN. The copolymer composition determination was achieved by SEC technique with RI and UV detectors. The reactivity ratios of the copolymers were estimated using four different linear graphical methods. The four methods gave close results, showing that curve fitting is enough to give a very good approximation of the reactivity ratios. The r_A values were weaker than the corresponding r_B values in all cases, meaning that a kinetic preference existed for the incorporation of B in the copolymer structure. Mean reactivity ratios of 0.55 and 12.3 were obtained for A and B, respectively. Eventually, from the calculations of dyad AA and BB probabilities, it has been possible to predict the copolymer composition dependence with the initial feed. To avoid long B sequences as requested for our diode application, the initial feed should not contain more than 5% of B.

Acknowledgements

We gratefully acknowledge Gérald Clisson and Abdel Khoukh, respectively, for SEC and NMR measurements. CNRS and Conseil Régional d'Aquitaine are thanked for the funding of Audrey Lateulade.

References

[1] Hoegl H. J Phys Chem 1965;69:755.
[2] Johnson GE. J Chem Phys 1975;62:4697.
[3] Davidson K, Soutar I, Swanson L, Yin J. J Polym Sci, Part B: Polym Phys 1997;35:963.
[4] Soutar I, Swanson L, Davidson K, Yin J. High Perform Polym 1997;9:353.
[5] Partridge RH. Polymer 1983;24:755.
[6] Kido J, Shionoya H, Nagai K. Appl Phys Lett 1995;67:2281.
[7] Zhang A, Von Seggern H, Pakbaz K, Kraabel B, Schmidt KHW, Heeger AJ. Synth Met 1994;62:35.
[8] Qiu Y, Duan L, Hu X, Zhang D, Zhang M, Bai F. Synth Met 2001;123:39.
[9] Bevington JC, Dyball CJ, Leech J. Makromol Chem 1979;180:657.
[10] Bevington JC, Dyball CJ. J Chem Soc, Faraday Trans 1975;1(71):2226.
[11] Penwell RC, Ganguly BN, Smith TW. J Polym Sci Macromol Rev 1978;13:63.
[12] Bevington JC, Dyball CJ. J Polym Sci Polym Chem Ed 1976;14:1819.
[13] Trathnigg B. Prop Polym Sci 1995;20:615.
[14] Philipsen HJA. J Chromatogr A 2004;1037:329.
[15] Thévenot C, Grassl B, Bastiat G, Binana W. Colloid Surf A: Physicochem Eng Aspects 2005;252:105.
[16] Brousseau J-L, Catalgil-Giz H, Reed WF. J Appl Sci 2000;77:3259.
[17] Brandrup J, Immergut EH.. 3rd ed Polymer Handbook.: Wiley; 1989.
[18] Mayo FR, Lewis FM. J Am Chem Soc 1974;96:4708.
[19] Finemann M, Ross S. J Polym Sci 1964;2:1687.
[20] Kelen T, Tüdos FJ. Macromol Sci 1975;9:1.
[21] Alfrey T, Goldfinger G. J Chem Phys 1944;12:205.
[22] Tazuke S, Nakagawa K, Okamura S. J Polym Sci, Part B 1965;3:923.
[23] Hart R. Makromol Chem 1961;47:143.
[24] Negulescu I, Feldmann D, Simionescu C. Polymer 1972;13:149.
[25] North AM, Whitlock KE. Polymer 1968;9:590.
[26] Candau F, François J, Benoît H. Polymer 1974;15:626.
[27] Kulicke WM, Kniewske R, Klein J. Progr Polym Sci 1982;8:373.
[28] Nathanson A. J Polym Sci, Part A: Polym Chem 1989;27:4257.
[29] Karali A, Froudakis GE, Dais P. Macromolecules 2000;33:3180.